metals

MDPI

Article

A Novel Turning-Induced-Deformation Based Technique to Process Magnesium Alloys

Sravya Tekumalla [1], Manasa Ajjarapu [2] and Manoj Gupta [1,*]

[1] Department of Mechanical Engineering, National University of Singapore, Singapore 117575, Singapore
[2] Department of Mechanical Engineering, Sastra Deemed University, Tamilnadu 613401, India
* Correspondence: mpegm@nus.edu.sg; Tel.: +65-6516-6358

Received: 9 July 2019; Accepted: 26 July 2019; Published: 29 July 2019



Abstract: A magnesium alloy was fabricated through the consolidation of chips accumulated during the turning process, followed by cold compaction and hot extrusion. A variation in the depths of cut was done during turning to understand the effect of deformation imparted during primary processing on the mechanical properties of an AZ91 alloy (Mg–9 wt.% Al–1 wt.% Zn–0.3 wt.% Mn). The results revealed a significant improvement in compressive strengths (up to 75%) with increased depth of cut, without compromising ductility through the development of fine-grained structures and prior plastic strain induction. This approach resulted in superior materials vis-a-vis conventional deformation techniques and promotes cost and energy efficiency through recycling industrial metal swarf, which is a significant environmental and economic concern.

Keywords: magnesium; turning; deformation; processing; strength

1. Introduction

For magnesium to replace the relatively heavier aluminum, titanium, and steels in structural applications, there are still several challenges that are persistent such as the inferior strength, ductility, corrosion resistance, etc. of magnesium [1]. Among the magnesium alloys, the most widely used commercial alloy AZ91 exhibits an excellent combination of mechanical properties, corrosion resistance, and cast ability [2]. However, improved strength is still needed to extend its applications. There have been several attempts made previously to improve its mechanical properties through altering the processing or modifying the alloy chemistry. The effectiveness of severe plastic deformation (SPD) techniques such as equal channel angular pressing (ECAP) to improve the mechanical properties of AZ91 alloy has been widely studied [3–5]. While this is a hot deformation technique, it was demonstrated that cold severe plastic deformation processes such as HPT (high pressure torsion) can render the AZ91 alloy superplastic [6]. Apart from these SPD techniques, effects of torsion deformation and ageing have also been studied [7] on age hardenable alloys such as the AZ91 alloy. It has been reported that this method was effective in reducing the yield asymmetry of the alloy, and deformation by torsion enhanced the effect of age-hardening that led to continuous precipitation, hence improving the mechanical properties of the alloy. Thus, significant enhancement of the properties can be achieved based on the extent of deformation introduced in the material. A majority of these deformation techniques are wrought techniques where the material undergoes secondary processing such as extrusion, rolling, or forging. In this work, the concept of deformation was used as an inspiration and applied as an extension to the primary processing to synthesize materials with better mechanical properties. In this regard, a novel approach of producing deformed material from chips/turnings obtained during the turning (machining) process followed by the conventional powder metallurgy of the turnings is proposed, as given in Figure 1. Turning of a metal involves the removal of material in the form of chips/turnings through localized deformation as stated in [8]. This approach of inducing

deformation is deemed to be an efficient form as it uses chips that are usually scrap formed during the removal of material to obtain the desired geometry. In the US, machining and other related operations accounts for an expenditure higher than hundred billion dollars ($100 billion) annually [9]. Most machine tools (>80%) typically used in the manufacturing industry are metal cutting in nature, leading to large volumes of metal swarf. Recycling these metal wastes could enhance economic profit and reduce the environmental impact of manufacturing (ore mining and metal refining to meet the metal stocks of global demand annually) [10]. Furthermore, due to the excellent machinability of most magnesium based materials, the machining of magnesium can be done via dry cutting where the need for cutting fluids or lubricants is eliminated before the recycling operation, thus making it an economical process [11]. Thus, this work proposed a novel, efficient, and economic approach of improving the mechanical properties of a magnesium alloy through a turning-induced-deformation technique. The as-cast ingots used in this work for turning and the generation of chips as several die cast magnesium alloys were machined to obtain the required dimensions and surface finish, and the magnesium swarf was generated in this process [12]. Although previous works have been undertaken on the consolidation of chips (solid state recycling) of magnesium, aluminum, and copper [13,14], there has been no systematic study, to the authors' best knowledge, on the properties of magnesium alloy-based chips, especially in light of the deformation imparted to the material based on the variation of the machining parameters. Furthermore, this work aimed to give direction to the solid-state recycling of chips generated not just through turning, but through all machining processes in general.

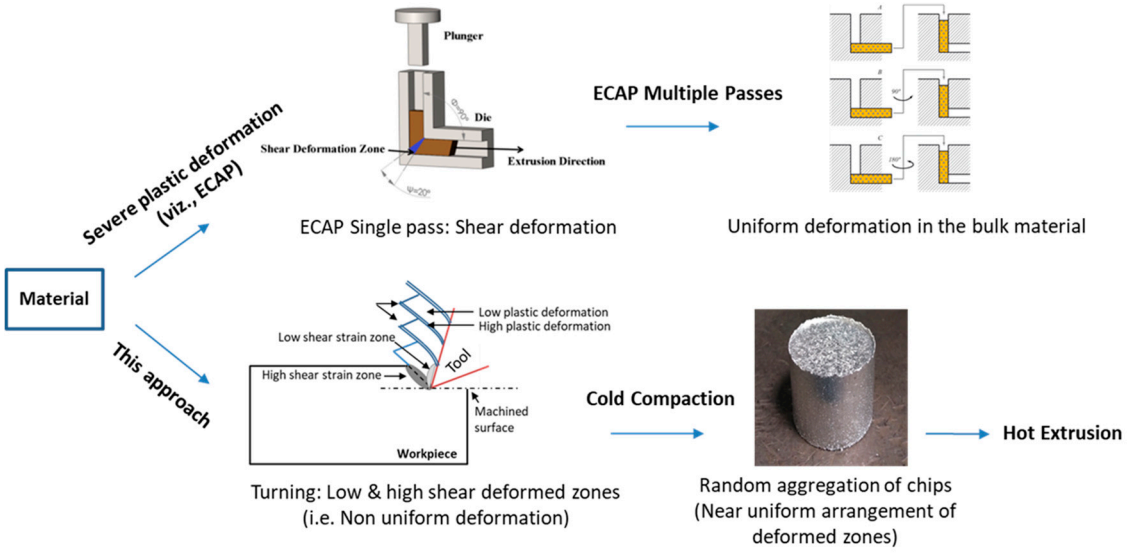


Figure 1. Mechanism of this approach vs. ECAP (equal channel angular pressing).

2. Materials and Methods

2.1. Processing

In this study, AZ91 alloys, supplied by Tokyo Magnesium Co. Ltd. (Yokohama, Japan), were used as the base materials. The AZ91 ingots were subjected to a turning operation performed on a lathe machine at 395 rpm and a feed rate of 62 mm/min. In this operation, a piece of material in the form of chips/turnings was removed from the surfaces of the work-piece/ingot using a carbide insert (TNMG 160404-HQ; Grade CA515, Hare & Forbes machinery house, Sydney, Australia) in a turning tool holder (Model No. WTJNR-2020-K16, Hare & Forbes machinery house, Sydney, Australia) with a tool height of 20 mm. The parameter that varied in the turning operation was the depth of cut (DOC) where the ingots were given three different DOCs: 0.5 mm DOC, 1.0 mm DOC, and 1.5 mm DOC, while all of the other parameters were kept constant. Compaction of the collected turnings was done uniaxial at room temperature in a hydraulic press for a duration of 1 min at a pressure of

1000 psi. The resultant compacted billets were then retrieved and soaked at 250 °C for 1 h before undergoing secondary thermo-mechanical processing. A 150-ton hydraulic press was used for the thermo-mechanical processing (hot extrusion) at a die temperature of 250 °C, resulting in rods of 8 mm in diameter. During extrusion, colloidal graphite aided as a lubricating agent. These rods, obtained from billets of 0.5 mm DOC turnings, 1 mm DOC turnings, and 1.5 mm DOC turnings were nomenclated as AZ91_0.5DOC, AZ91_1DOC, and AZ91_1.5DOC, respectively, in this study. Furthermore, as a benchmark, the AZ91 ingot was also extruded directly, without turning, at the same parameters and henceforth termed as AZ91_AR (where AR stands for As Received) and served as the comparative base material/benchmark.

2.2. Density and Porosity Measurements

The density of the samples was measured using the Archimedes' principle. The weights of the samples were measured using an ER-182A electronic balance (A&D Engineering, Thebarton, Australia) with an uncertainty of ±0.0001 g. The densities were also measured using a gas pycnometer where an inert gas (helium) was used as the displacement medium and the values were cross checked. Porosity of the samples was measured using the theoretical and experimental densities under the assumption that the discrepancies between the theoretical and experimental densities were due to the porosity of the material.

2.3. Microstructure and X-Ray Diffraction

Grain characteristics were computed using the line intercept method following ASTM E112–13 standards on images obtained from the scanning electron microscope (SEM). Microstructural characterization was performed through SEM (JEOL-JSM-6010, Jeol USA Inc., Peabody, MA, USA) with an attached EDS (energy dispersive spectrometry) analysis. Furthermore, secondary phase analysis was done on an automated Shimadzu-LAB XRD series 6000 using a Cu Kα radiation of wavelength 1.54 A° at a scan speed of 2°/min.

2.4. Mechanical Characterization

Micro-hardness was measured with the aid of a digital micro-hardness tester (Shimadzu (Asia Pacific) Pte Ltd, Singapore, Singapore) in accordance with ASTM E384-11e1 (245.5 mN of load; 15 s of dwell time). Compressive loading using a servo-hydraulic fully automated mechanical testing machine (Eden Prairie, MN, USA), MTS 810, was done uniaxial following the ASTM E9-09 standard at a quasi-static strain rate of 1.6×10^{-4} s^{-1}.

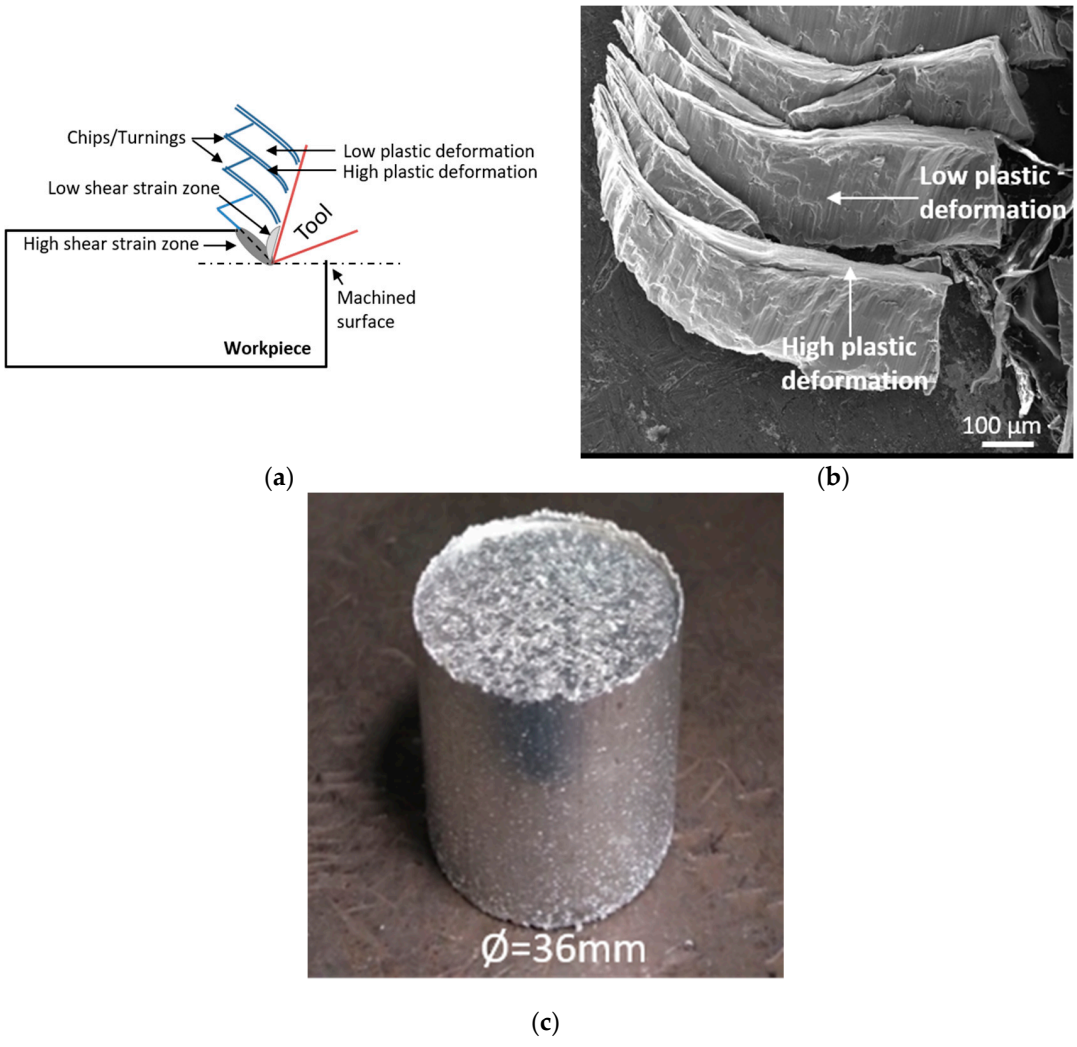
3. Results and Discussion

3.1. Plastic Deformation Induced during Turning

When the as-received ingots were subjected to turning, the work-piece/metal underwent a material removal process by a sharp cutting tool. This cutting action involved two main steps: (i) formation of a chip, which happens through a localized shear process in a narrow region where the metal is compressed; and then (ii) the metal is made to flow on the face of the tool. Chip formation involves the work material to be deformed by shear, and as chips are removed, new surfaces are exposed to the tool. Figure 2a gives a realistic view of chip formation, showing two distinct shear deformation zones i.e., a high shear strain zone at the tool-work-piece interaction, resulting in high plastic deformation and a low shear strain zone due to the tool-chip friction resulting in a low plastic deformation of the chip. Figure 2b validates this by demonstrating the presence of shear bands on the chips at the two zones marked as low and high plastic deformation zones. The image was taken from a section of the chips randomly. It may be noted that the materials with increased depths of cut appeared to have more discontinuous chips. With an increment in the depths of cut from 0.5 mm to 1.5 mm progressively, the material removal rate (which is directly proportional to the depth of cut) was increased, implying the

increase in the extent of deformation in the materials. Thus, it can be noted that materials with 1.5 mm DOC have chips that imparted a higher degree of shear deformation when compared to the material with 0.5 mm and 1 mm DOCs [9].

These turnings were then consolidated and subjected to cold compaction, like the powder metallurgy route, to obtain a billet (Figure 2c) that was then soaked and hot extruded. During soaking, the mechanically bonded turnings in the billet softened due to the raised temperature of soaking (250 °C) and fused together to form bonds under the influence of high temperature. This process is thought to be like the process of sintering, where green compacts are heated below the melting temperature of the metal to fuse the particles together. Although, in the current scenario, a soaking temperature of 250 °C would not entirely suffice to completely fuse the turnings together, hot extrusion (a process that involves high temperatures as well as pressure) helps accelerate this process to obtain a well fused bulk metal product.



(**a**) (**b**)

(**c**)

Figure 2. (**a**) Chip formation during turning; (**b**) chips/turnings (Depth of cut DOC of 1.5 mm) with apparent plastic deformation zones; (**c**) turnings compacted into a billet.

3.2. *Effect of Deformation on Microstructural Features*

The results of the density and porosity measurements of the extruded materials are given in Table 1. The theoretical density of the AZ91 alloy was 1.835 g/cc. The AZ91_AR material i.e., the extruded-as received material had an experimental density of 1.816 g/cc with a porosity of 1.06%. It was observed that the DOC materials also exhibited a similar range of porosity with almost no deviation

when compared to the AZ91_AR material. This shows that the consolidation of the chips and hot extrusion helped in the elimination of porosity in the final material. Thus, the effects of porosity or voids in the materials on the properties can be considered negligible.

Table 1. Density and porosity results.

Composition	Experimental Density (g/cm^3)	Theoretical Density (g/cm^3)	Porosity (%)
AZ91_AR	1.816	1.835	1.06
AZ91_0.5 DOC	1.815	1.835	1.10
AZ91_1 DOC	1.812	1.835	1.27
AZ91_1.5 DOC	1.817	1.835	1.02

The microstructures (along the longitudinal section) revealed very fine recrystallized grains for all of the materials (Figure 3a–d), particularly the ones with prior induced deformation (turning). However, all materials exhibited a bimodal grain structure i.e., bands of dynamically recrystallized (DRXed) and elongated worked grains. Figure 3 indicates that with an increase in deformation in the material during turning (DOC), the average DRXed grain size decreased progressively. AZ91_1.5DOC exhibited the lowest DRXed grain size (1.27 µm), which was 60% lower than that of the AZ91_AR.

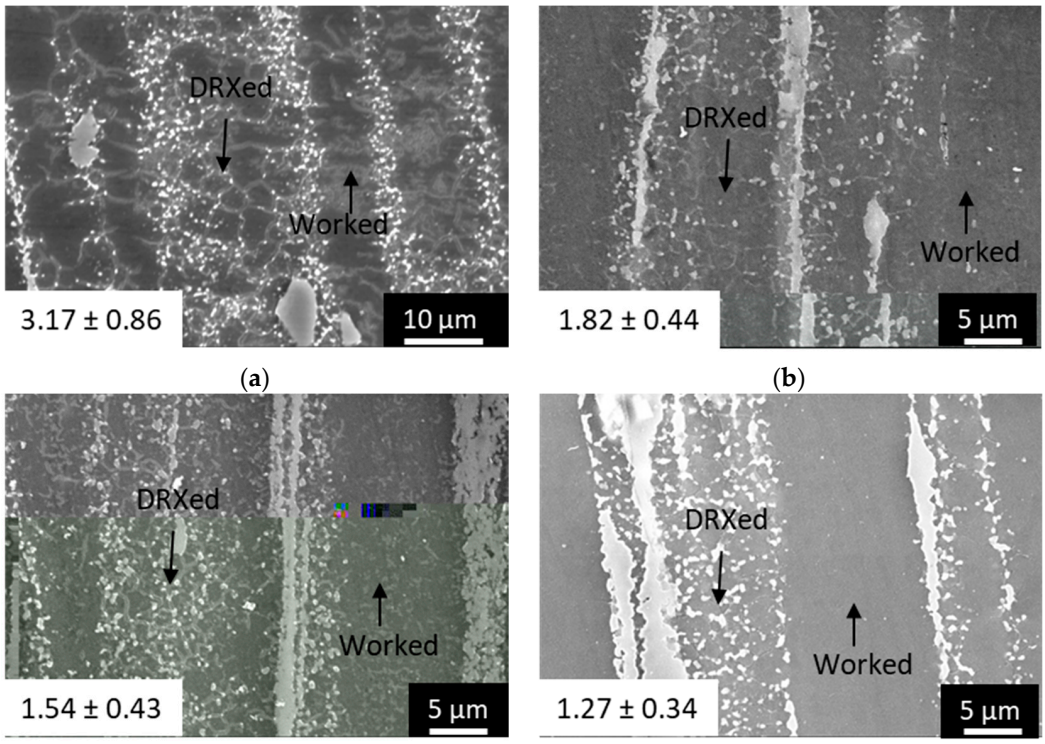


Figure 3. Microstructure of (**a**) AZ91_AR; (**b**) AZ91_0.5DOC; (**c**) AZ91_1DOC; and (**d**) AZ91_1.5DOC alloys with insets of average DRXed values.

The individual chips shown in Figure 2b were subjected to XRD to identify the presence of phases prior to compaction and extrusion. The results in Figure 4a show that the materials comprised of α-Mg and $Mg_{17}Al_{12}$ phases in the as-received condition as well as in the 0.5, 1, and 1.5 DOC turnings/chips. Compared to the as-received material in the ingot condition, the normalized intensity of $Mg_{17}Al_{12}$ peaks in the turnings was much lower, particularly at an angle of ~36°. This is believed to be due to the reduction in the size of the phases, thereby changing their distribution due to the processing that led to the drop in the intensity from the corresponding phase when subjected to x-ray

diffraction. Furthermore, the XRD of AZ91 in the as-received condition revealed the lowest intensity at 34° (corresponding to the (0001) basal plane), indicating a strong basal texture. However, it is to be noted that the turnings did not exhibit any dominant texture as seen from their intensities due to the random selection of differently oriented turnings for XRD. Figure 4b also provides a qualitative idea about the texture of the materials. All the materials exhibited a strong texture with the intensity at 2 Theta of 34° corresponding to the basal plane, being the lowest in the XRD of the cross section of the samples. Although there could be a variation in the texture strengths, it was noted that all the materials exhibited a strong extrusion texture.

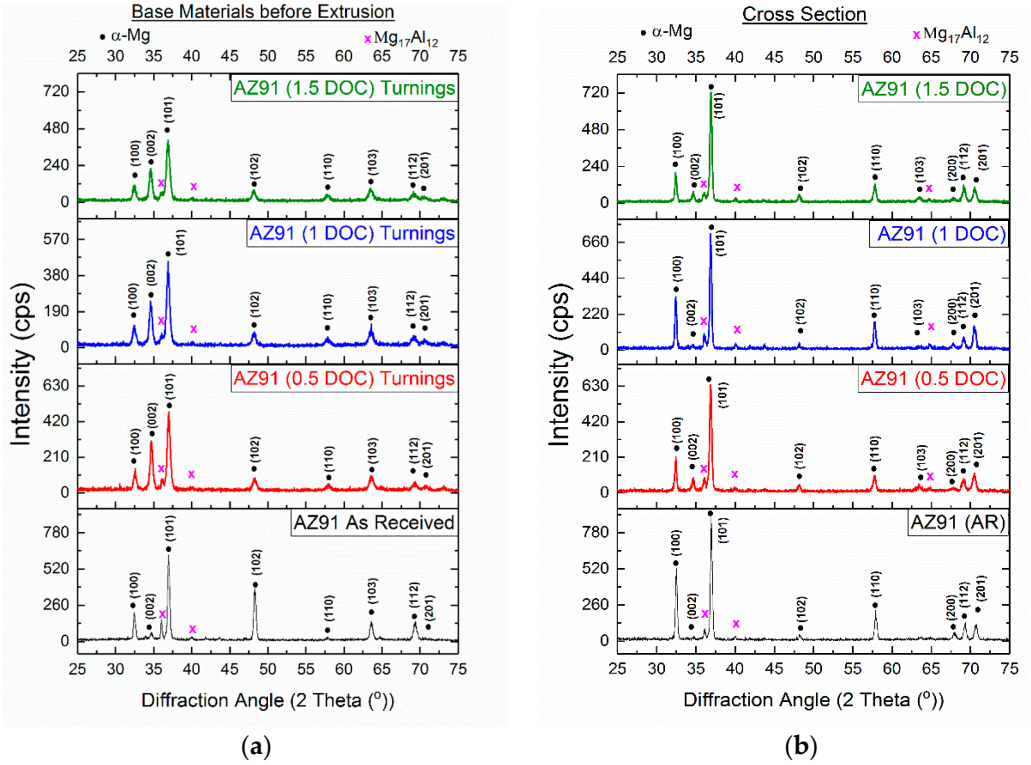


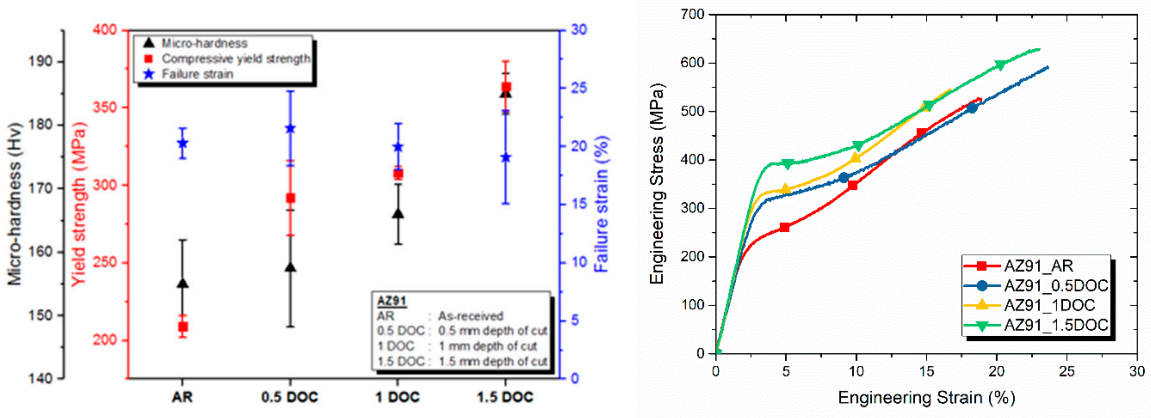
Figure 4. XRD of (**a**) base materials i.e., turnings/chips before extrusion, and (**b**) extruded materials.

Furthermore, SEM images (Figure 3a–d) and XRD (Figure 4) revealed that the materials contained α-Mg + $Mg_{17}Al_{12}$ phases distributed across the microstructure. For recrystallization to occur, adequate prior deformation to provide nuclei and sufficient stored energy to drive their growth is necessary. Increasing the deformation, i.e., by increasing the depth of cut in this case, increases the rate of nucleation faster than it increases the rate of growth [15]. Therefore, the final DRXed grain size reduces with increased deformation, as was the case for AZ91_1.5DOC. However, the presence of phases also affects the final grain size. Increased presence of continuous bands of precipitates was observed in the AZ91_DOC alloy compared to AZ91_AR. This suppressed the complete nucleation of new grains during extrusion in the deformed alloys, resulting in the presence of high amounts of worked grains, which was also expressed previously in [7].

3.3. Effect of Deformation on Mechanical Properties

The micro-hardness and compressive properties are given in Figure 5a. A general observation was made that the micro-hardness of those materials with induced deformation was higher than that of the material that was not imparted with any prior deformation. Furthermore, with increase in the deformation (i.e., increased DOC), the micro-hardness increased significantly to as high as 185 HV in AZ91_1.5DOC. The compressive yield strength followed a similar trend as that of micro-hardness, i.e., the compressive yield strength progressively increased with increments in DOC as seen in Figure 5b.

AZ91_1.5DOC exhibited the highest compressive yield strength of about 364 MPa, which was 75% higher than that of AZ91_AR. This shows the significance of this method in imparting strength to the material. Furthermore, the strains to failure were in the same range as that of the as received condition, with all the materials exhibiting a reasonable failure strain of >15%, indicating no compromise in the ductility of the materials under compressive loading.



(**a**) (**b**)

Figure 5. (**a**) Mechanical properties of materials; and (**b**) representative engineering stress-strain curves of the materials.

The remarkable increment in the compressive yield strength in the DOC materials as against the as received (AZ91_AR) was due to a few critical factors. One such factor is the development of fine-recrystallized grained structures in DOC materials compared to AR, which helps in improving the yield strength following the Hall–Petch equation [16,17]. This was substantiated by AZ91_1.5DOC exhibiting a grain size 60% smaller than that of the AR alloy and a yield strength 75% higher than the AR alloy. Furthermore, the prior deformation in the turnings resulted in strain hardened materials when compared to the as received material. Strain hardening, therefore, is another dominating strengthening mechanism that was responsible for AZ91_1.5DOC exhibiting a high compressive yield strength. Thus, this significant enhancement in the mechanical properties of the materials can be attributed to their grain structure, which is also correlated to the extent of prior deformation during turning (in the form of increasing DOCs). Another possible mechanism is the dispersion strengthening of magnesium by the oxides [18] stemming from the surface of the chips. However, this needs further study and understanding before conclusive remarks can be made as to whether the size of the oxides plays a crucial role in the strengthening mechanism. Furthermore, the oxide size also affects the ductility. Hence, it is the future scope of this work to identify the isolated contribution of such a mechanism.

3.4. Mechanism and Comparison with Conventional Deformation Processes

This turning induced deformation approach was compared to the conventional cold deformation techniques such as torsion induced deformation, which was undertaken by [7], to understand the effectiveness of this approach. Figure 6 gives the mechanical properties of the same AZ91 alloy processed through this approach and the torsion induced deformation approach. In the torsion-induced deformation approach, the materials were solution treated for 3 h at 420 °C and extruded at 400 °C and then subjected to free end torsion deformation. Although the processing and the process parameters differed from this work, the two types of deformation were done on the same material (i.e., AZ91) and were compared in terms of their compressive properties. It was evident that the yield strength of AZ91_1.5DOC was about 45% higher than that of the torsion deformed and aged AZ91, indicating the effectiveness of this technique in improving strength. Furthermore, a mechanism of this approach was established alongside a comparison to the conventional SPD techniques such as ECAP (Figure 1). ECAP usually results in a uniform deformation of bulk material after multiple passes [3], with a high amount

of strain imparted to the material. This results in a tremendous improvement in the properties of the material that is processed by ECAP. While this technique initially imparts a non-uniform deformation (localized primary and secondary plastic deformation zone) in each chip, however, this non-uniform deformation is overcome by the consolidation of randomly oriented (Figure 2c) and deformed chips during compaction, which leads to a rather uniform arrangement of chips; in other words, a near uniform deformation of the bulk material similar to that of ECAP occurs. It must be noted that the amount of strain imparted in ECAP is much higher than the current technique and was used only as a means of comparison. Thus, this technique is highly effective in imparting near-uniform deformation and strength to magnesium alloys. However, one limitation with this technique is that the total volume of the resultant extruded material is lower when compared to an extrudate of a cast billet because of the air pockets between the chips in the consolidated billet. Furthermore, other secondary deformation methods like rolling or swaging could also lead to similar improvements in the mechanical properties, which would be an interesting direction of research to recycle magnesium alloys and composites.

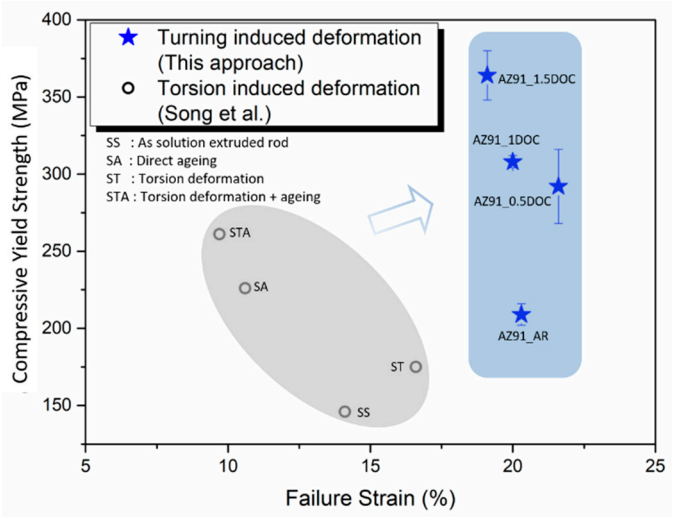


Figure 6. Comparison between turning-induced and torsion-induced deformation.

4. Conclusions

AZ91 alloys were successfully fabricated through the consolidation of chips formed during turning, followed by cold compaction and hot extrusion. This work revealed that the increase in depth of cut during turning imparted a higher amount of deformation in the chips, resulting in improved hardness and compressive strengths of AZ91 alloy. A maximum compressive yield strength of 364 MPa was observed in the AZ91_1.5DOC alloy, which was 75% higher than the AZ91_AR alloy. This was due to the development of fine-grained structures in the AZ91_1.5DOC alloy, which were 60% smaller than that of the AZ91_AR alloy as well as the plastic deformation induced in the chips during turning that resulted in strain hardening. This turning-induced-deformation technique, in addition to conventional deformation routes (such as torsion), is a viable route for the strengthening of Mg alloys.

Author Contributions: Conceptualization and design of experiments, S.T. and M.G.; Performed the experiments and analyzed the data, S.T. and M.A.; Writing—original draft preparation, S.T.; Writing—review and editing, S.T. and M.G.; Project administration, S.T.; Funding acquisition, M.G.

Funding: This research was funded by the Ministry of Education, Singapore, grant number R 265 000 622 112.

Acknowledgments: The authors would like to thank Juraimi Bin Madon for his assistance in extruding all of the materials.

Conflicts of Interest: The authors declare no conflicts of interest.

References

1. Tekumalla, S.; Nandigam, Y.; Bibhanshu, N.; Rajashekara, S.; Yang, C.; Suwas, S.; Gupta, M. A strong and deformable in-situ magnesium nanocomposite igniting above 1000 °C. *Sci. Rep.* **2018**, *8*, 7038. [CrossRef] [PubMed]
2. Chung, C.W.; Ding, R.G.; Chiu, Y.L.; Gao, W. Effect of ECAP on microstructure and mechanical properties of cast AZ91 magnesium alloy. *J. Phys. Conf. Ser.* **2010**, *241*, 012101. [CrossRef]
3. Bryła, K.; Dutkiewicz, J.; Litynska-Dobrzynska, L.; Rokhlin, L.L.; Kurtyka, P. Influence of number of ECAP passes on microstructure and mechanical properties of AZ31 magnesium alloy. *Arch. Metall. Mater.* **2012**, *57*, 711–717. [CrossRef]
4. Sun, J.; Yang, Z.; Han, J.; Liu, H.; Song, D.; Jiang, J.; Ma, A. High strength and ductility AZ91 magnesium alloy with multi-heterogenous microstructures prepared by high-temperature ECAP and short-time aging. *Mater. Sci. Eng. A* **2018**, *734*, 485–490. [CrossRef]
5. Yuan, Y.; Ma, A.; Jiang, J.; Lu, F.; Jian, W.; Song, D.; Zhu, Y.T. Optimizing the strength and ductility of AZ91 mg alloy by ECAP and subsequent aging. *Mater. Sci. Eng. A* **2013**, *588*, 329–334. [CrossRef]
6. Al-Zubaydi, A.S.J.; Zhilyaev, A.P.; Wang, S.C.; Reed, P.A.S. Superplastic behaviour of AZ91 magnesium alloy processed by high-pressure torsion. *Mater. Sci. Eng. A* **2015**, *637*, 1–11. [CrossRef]
7. Song, B.; Wang, C.; Guo, N.; Pan, H.; Xin, R. Improving tensile and compressive properties of an extruded AZ91 rod by the combined use of torsion deformation and aging treatment. *Materials* **2017**, *10*, 280. [CrossRef] [PubMed]
8. Ghadbeigi, H.; Bradbury, S.R.; Pinna, C.; Yates, J.R. Determination of micro-scale plastic strain caused by orthogonal cutting. *Int. J. Mach. Tools Manuf.* **2008**, *48*, 228–235. [CrossRef]
9. Sinha, N. *Ta202a: Introduction to Manufacturing Processes*; Department of Mechanical Engineering, IIT Kanpur: Kanpur, India, 2017.
10. Xiong, B.; Zhang, X.; Li, F.; Hu, H.; Liu, C. Recycling of aluminum A380 machining chips. In *Light Metals 2015*; Hyland, M., Ed.; Springer International Publishing: Cham, Switzerland, 2016; pp. 1011–1015.
11. Guo, Y.B.; Salahshoor, M. Process mechanics and surface integrity by high-speed dry milling of biodegradable magnesium–calcium implant alloys. *CIRP Ann.* **2010**, *59*, 151–154. [CrossRef]
12. ASM International. Machining of magnesium and magnesium alloys. In *Machining*; ASM International: Materials Park, OH, USA, 1989; Volume 16.
13. Wan, B.; Chen, W.; Lu, T.; Liu, F.; Jiang, Z.; Mao, M. Review of solid state recycling of aluminum chips. *Resour. Conserv. Recycl.* **2017**, *125*, 37–47. [CrossRef]
14. Hu, M.-L.; Ji, Z.-S.; Chen, X.-Y.; Wang, Q.-D.; Ding, W.-J. Solid-state recycling of AZ91D magnesium alloy chips. *Trans. Nonferrous Met. Soc. China* **2012**, *22*, s68–s73. [CrossRef]
15. Rios, P.R.; Siciliano, F., Jr.; Sandim, H.R.Z.; Plaut, R.L.; Padilha, A.F. Nucleation and growth during recrystallization. *Mater. Res.* **2005**, *8*, 225–238. [CrossRef]
16. Yang, W.; Tekumalla, S.; Gupta, M. Cumulative effect of strength enhancer—lanthanum and ductility enhancer—cerium on mechanical response of magnesium. *Metals* **2017**, *7*, 241. [CrossRef]
17. Chen, Y.; Tekumalla, S.; Guo, Y.B.; Shabadi, R.; Shim, V.P.W.; Gupta, M. The dynamic compressive response of a high-strength magnesium alloy and its nanocomposite. *Mater. Sci. Eng. A* **2017**, *702*, 65–72. [CrossRef]
18. Tekumalla, S.; Shabadi, R.; Yang, C.; Seetharaman, S.; Gupta, M. Strengthening due to the in-situ evolution of ß1′ Mg-Zn rich phase in a ZnO nanoparticles introduced Mg-Y alloy. *Scr. Mater.* **2017**, *133*, 29–32. [CrossRef]



© 2019 by the authors. Licensee MDPI, Basel, Switzerland. This article is an open access article distributed under the terms and conditions of the Creative Commons Attribution (CC BY) license (http://creativecommons.org/licenses/by/4.0/).